Metal- *versus* Ligand-Centered Oxidations in Phenolato−Vanadium and −Cobalt Complexes: Characterization of Phenoxyl−Cobalt(III) Species

Achim Sokolowski, Britta Adam, Thomas Weyhermüller, Akihiro Kikuchi, Knut Hildenbrand, Robert Schnepf, Peter Hildebrandt, Eckhard Bill, and Karl Wieghardt*

Max-Planck-Institut für Strahlenchemie, D-45470 Mülheim an der Ruhr, Germany

Received March 4, 1997[⊗]

The coordination chemistry of the pendent-arm macrocycles 1,4,7-tris(3,5-dimethyl-2-hydroxybenzyl)-1,4,7-triazacyclononane, $L^{Me}H_3$, 1,4,7-tris(3,5-di-*tert*-butyl-2-hydroxybenzyl)-1,4,7-triazacyclononane, $L^{Bu}H_3$, 1,4,7-tris(3-*tert*-butyl-5-methoxy-2-hydroxybenzyl)-1,4,7-triazacyclononane, $L^{OCH_3}H_3$, and Tolman's ligand 1,4-diisopropyl-7-(3,5-di-*tert*-butyl-2-hydroxybenzyl)-1,4,7-triazacyclononane, $L^{Pr}H$, with vanadium and cobalt(III) has been studied. The following complexes containing a *fac*-N_3O_3 donor set have been synthesized: $[L^{Me}V^{III}]$ (**1**), $[L^{Me}V^{IV}]PF_6$ (**2**), $[(L^{Me}H)V^{V}(O)]PF_6$ (**3**), $[L^{Bu}V^{IV}]PF_6$ (**4**), $[L^{OCH_3}V^{IV}]PF_6$ (**5**), $[L^{Me}Co^{III}]$ (**6**), $[L^{Bu}Co^{III}]$ (**7**), $[L^{OCH_3}Co^{III}]$ (**8**). In addition, two complexes containing the $L^{Pr}Co^{III}$ fragment have been prepared: $[L^{Pr}Co^{III}(acac)](ClO_4)$ (**9**) and $[L^{Pr}Co^{III}(Cl_4cat)]\cdot CH_3CN$ (**10**), where $acac^-$ represents the ligand pentane-2,4-dionate and Cl_4cat^{2-} is tetrachlorocatecholate. Complexes **9** and **10** have been characterized by single-crystal X-ray crystallography: **9** crystallizes in the triclinic space group $P\bar{1}$ with $a = 9.493(1)$ Å, $b = 9.760(1)$ Å, $c = 18.979(2)$ Å, $\alpha = 88.57(1)°$, $\beta = 78.60(1)°$, $\gamma = 79.24(1)°$, $V = 1693.3(3)$ Å^3, and $Z = 2$; **10** crystallizes in the monoclinic space group $P2_1/n$ with $a = 10.184(2)$ Å, $b = 24.860(5)$ Å, $c = 14.872(3)$ Å, $\beta = 97.95(3)°$, $V = 3729(1)$ Å^3, and $Z = 4$. Electrochemically, complexes **2**, **4**, and **5** can be reversibly oxidized by one electron, yielding vanadium(V), and one-electron-reduced, affording vanadium(III) species; **3** can be reduced to $[L^{Me}HV^{IV}(O)]$. These redox processes are shown to be metal-centered. In contrast, the cyclic voltammograms of **7** and **8** display *three* reversible one-electron oxidations. For the monocations $[\mathbf{7}]^{\bullet+}$ and $[\mathbf{8}]^{\bullet+}$, EPR and UV−vis spectroscopies reveal that these are phenoxyl−cobalt(III) species. Thus, the redox processes are ligand-centered. Similarly, $[\mathbf{9}]^+$ is reversibly oxidized to the phenoxyl−cobalt(III) complex $[\mathbf{9}]^{\bullet 2+}$ ($S = {}^1/_2$). For **10**, two reversible one-electron oxidation steps have been identified generating $[\mathbf{10}]^{\bullet+}$ ($S = {}^1/_2$) and $[\mathbf{10}]^{2\bullet 2+}$ ($S = 1$). It is unambiguously shown by EPR and resonance Raman spectroscopies that $[\mathbf{10}]^{\bullet+}$ contains a (phenolato)(semiquinonato)cobalt(III) unit whereas in $[\mathbf{10}]^{2\bullet 2+}$ a phenoxyl(semiquinonato)cobalt(III) unit prevails.

Introduction

Pendent-arm macrocyclic ligands derived from N-functionalized 1,4,7-triazacyclononane[1−6] have been shown to form extremely stable[7,8] first-row transition metal complexes. In recent years, the coordination chemistry of the tris(*N*-phenolato)-pendent-arm derivatives has been extensively studied.[1−8] For example, we have been able to show[4] that the potassium salt of 1,4,7-tris(5-*tert*-butyl-2-hydroxybenzyl)-1,4,7-triazacyclononane, $K_3[L]$, reacts with VCl_3 in acetonitrile quantitatively to yield $[LV^{III}]$. Electrochemically, this species can be reversibly *oxidized*, generating successively $[LV^{IV}]^+$ and $[LV^{V}]^{2+}$, and *reduced* at very negative potentials to the monoanion $[LV^{II}]^-$. Thus, *four* oxidation states of the central metal ion are available without changing the ligand environment comprising a *fac*-N_3O_3 donor set.

In contrast, we have recently shown[10] that, by protecting the ortho and para positions of the phenolate pendent arms by bulky substituents such as *tert*-butyl groups and introducing a redox-inactive metal ion such as Ga^{III}, Sc^{III}, or Zn^{II},[11] it is possible to successively and reversibly oxidize the three phenolato ligands in $[L^{Bu}M]$ (M = Ga, Sc) or $[LZn^{II}]^-$ to give relatively stable phenoxyl radical complexes. $[L^{Bu}]^{3-}$ represents the trianion of 1,4,7-tris(3,5-di-*tert*-butyl-2-hydroxybenzyl)-1,4,7-triazacyclononane (see Chart 1). Thus, the monocation $[L^{Bu}Ga]^{\bullet+}$, the dication $[L^{Bu}Ga]^{2\bullet 2+}$, and the trication $[L^{Bu}Ga]^{3\bullet 3+}$ contain one, two, and three coordinated phenoxyl ligands, respectively. In this instance, ligand-centered redox processes prevail.

In essence, this work has shown that phenolates belong to the growing class of noninnocent ligands. For a given transition metal complex of this type, it is therefore not possible to *a priori* assign an oxidation state to the metal ion involved with d^n electron configuration.

This dichotomy plays an important role in some copper-containing metalloproteins such as galactose oxidase[12] and glyoxal oxidase,[13] for which the active forms have been shown

⊗ Abstract published in *Advance ACS Abstracts,* August 1, 1997.

(1) Moore, D. A.; Fanwick, P. E.; Welch, M. J. *Inorg. Chem.* **1989**, *28*, 1504.
(2) Auerbach, U.; Eckert, U.; Wieghardt, K.; Nuber, B.; Weiss, J. *Inorg. Chem.* **1990**, *29*, 938.
(3) Martell, A. E.; Motekaitis, R. J.; Welch, M. J. *J. Chem. Soc., Chem. Commun.* **1990**, 1748.
(4) Auerbach, U.; Della Vedova, S. P. C.; Wieghardt, K.; Nuber, B.; Weiss, J. *J. Chem. Soc., Chem. Commun.* **1990**, 1004.
(5) Auerbach, U.; Stockheim, C.; Weyhermüller, T.; Wieghardt, K.; Nuber, B. *Angew. Chem.* **1993**, *105*, 735; *Angew. Chem., Int. Ed. Engl.* **1993**, *32*, 714.
(6) Auerbach, U.; Weyhermüller, T.; Wieghardt, K.; Nuber, B.; Bill, E.; Butzlaff, C.; Trautwein, A. X. *Inorg. Chem.* **1993**, *32*, 508.
(7) Clarke, E. T.; Martell, A. E. *Inorg. Chim. Acta* **1991**, *186*, 103.
(8) Martell, A. E.; Motekaitis, R. J.; Welch, M. J. *J. Chem. Soc., Chem. Commun.* **1990**, 1748.
(9) Motekaitis, M. J.; Sun, Y.; Martell, A. E. *Inorg. Chim. Acta* **1992**, *198−200*, 421.
(10) Adam, B.; Bill, E.; Bothe, E.; Goerdt, B.; Haselhorst, G.; Hildenbrand, K.; Sokolowski, A.; Steenken, S.; Weyhermüller, T.; Wieghardt, K. *Chem. Eur. J.* **1997**, *3*, 308.
(11) Sokolowski, A.; Müller, J.; Weyhermüller, T.; Schnepf, R.; Hildebrandt, P.; Hildenbrand, K.; Bothe, E.; Wieghardt, K. *J. Am. Chem. Soc.*, in press.
(12) (a) Ettinger, J. E.; Kosman, D. J. In *Copper Proteins*; Spiro, T. G., Ed.; Wiley and Sons: New York, 1981; p 221. (b) Whittaker, J. W. In *Metal Ions in Biological Systems*; Sigel, H., Sigel, A., Eds.; Marcel Dekker: New York, 1994; Vol. 30, p 315.
(13) Whittaker, M. W.; Kersten, P. J.; Nakamura, N.; Sanders-Loehr, J.; Schweizer, E. S.; Whittaker, J. W. *J. Biol. Chem.* **1996**, *271*, 681.

S0020-1669(97)00256-5 CCC: $14.00

Chart 1. Ligands and Complexes

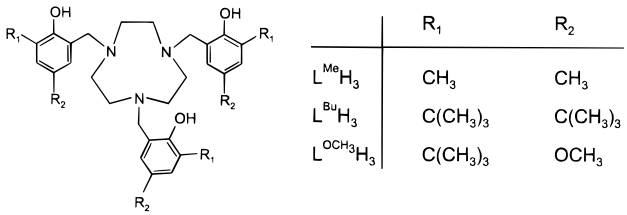

	R_1	R_2
$L^{Me}H_3$	CH_3	CH_3
$L^{Bu}H_3$	$C(CH_3)_3$	$C(CH_3)_3$
$L^{OCH_3}H_3$	$C(CH_3)_3$	OCH_3

$[L^{Me}V^{III}]$	**1**	$[L^{Me}Co^{III}]$	**6**
$[L^{Me}V^{IV}]PF_6$	**2**	$[L^{Bu}Co^{III}]$	**7**
$[(L^{Me}H)V^{V}O]PF_6$	**3**	$[L^{OCH_3}Co^{III}]$	**8**
$[L^{Bu}V^{IV}]PF_6$	**4**		
$[L^{OCH_3}V^{IV}]PF_6$	**5**		

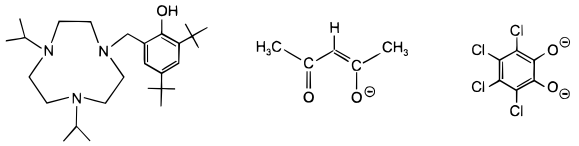

$L^{Pr}H$ $acac^-$ $Cl_4\text{-}cat^{2-}$

$[L^{Pr}Co^{III}(acac)](ClO_4)$ **9**

$[L^{Pr}Co^{III}(Cl_4\text{-}cat)]CH_3CN$ **10**

by spectroscopic methods (UV−vis, resonance Raman, EPR, and EXAFS) to contain a tyrosyl−copper(II) rather than a tyrosinate−copper(III) unit.

In this work, we describe the coordination and redox chemistry of the pendent-arm macrocycles $L^{Me}H_3$,[1] $L^{Bu}H_3$,[10] and $L^{OCH_3}H_3$,[10] the structures of which are depicted in Chart 1, with vanadium and cobalt(III). As we will show, the redox chemistry of the vanadium complexes **1**−**5** is metal-centered and that of the cobalt(III) complexes **6**−**8** is ligand-centered. We have also used the tetradentate ligand 1,4-diisopropyl-7-(3,5-*tert*-butyl-2-hydroxybenzyl)-1,4,7-triazacyclononane, $L^{Pr}H$, described recently by Tolman et al.,[14] and prepared the two complexes **9** and **10** containing the $L^{Pr}Co^{III}$ fragment and, in addition, the redox-innocent didentate ligand pentane-2,4-dionate, $acac^-$, or the potentially redox-active tetrachlorocatecholate dianion, Cl_4cat^{2-}.

The neutral complex **10** represents an interesting test case because both the catecholate and the phenolate can, in principle, undergo a ligand-centered one-electron oxidation, generating a coordinated semiquinonate and a coordinated neutral phenoxyl radical, respectively. As we show here, it is possible to discern unambiguously by spectroscopic methods (UV−vis, resonance Raman, and EPR) which of the two possible valence isomers is present in the monocation $[\mathbf{10}]^{\bullet+}$: the (phenolato)(semiquinonato)cobalt(III) or the phenoxyl(catecholato)cobalt(III) species. The corresponding dication $[\mathbf{10}]^{2\bullet 2+}$ contains a phenoxyl and a tetrachlorosemiquinonate ligand.

Experimental Section

Caution. Sodium perchlorate was used in the following syntheses. Perchlorate salts are potentially explosive and should be handled in small quantities and with appropriate precautions.

The ligands 1,4-diisopropyl-7-(3,5-di-*tert*-butyl-2-hydroxybenzyl)-1,4,7-triazacyclononane,[14] $L^{Pr}H$, 1,4,7-tris(3,5-dimethyl-2-hydroxybenzyl)-1,4,7-triazacyclononane,[1] $L^{Me}H_3$, 1,4,7-tris(3,5-di-*tert*-butyl-2-hydroxybenzyl)-1,4,7-triazacyclononane,[10] $L^{Bu}H_3$, and 1,4,7-tris(3-*tert*-butyl-5-methoxy-2-hydroxybenzyl)-1,4,7-triazacyclononane,[10] $L^{OCH_3}H_3$, were prepared according to published procedures.

Preparation of Complexes. $[L^{Me}V^{III}]$ (1). A deoxygenated solution of VCl_3 (0.16 g; 1.0 mmol) in CH_3CN (20 mL) was heated to reflux for 20 min under an argon atmosphere until a clear green solution of $[VCl_3(CH_3CN)_3]$ was obtained. Addition of $L^{Me}H_3$ (0.54 g; 1.0 mmol) and a few drops of triethylamine gave a deep green solution from which a microcrystalline green solid material slowly precipitated. Yield: 0.36 g (63%). μ_{eff}(293 K): 2.89 μ_B. FAB MS (MNBA): *m*/*z* 579.3 {$[M^+]$}. Anal. Calcd for $C_{33}H_{42}N_3O_3V$: C, 68.3; H, 7.4; N, 7.2. Found: C, 68.1; H, 7.6; N, 6.9.

$[L^{Me}V^{IV}]PF_6$ (2). To a solution of **1** (0.58 g; 1.0 mmol) in CH_3OH (30 mL) were added $Na_2S_2O_8$ (0.3 g) and one drop of concentrated $HClO_4$ with stirring at room temperature. The deep violet solution was filtered, and solid $NaPF_6$ (1.0 g) was added, which initiated the precipitation of violet microcrystals. Yield: 0.49 g (68%). μ_{eff}(293 K): 1.73 μ_B. FAB MS (MNBA): *m*/*z* 579.3 {$[M^+]$}. Anal. Calcd for $C_{33}H_{42}N_3O_3VPF_6$: C, 54.7; H, 5.8; N, 5.8. Found: C, 54.5; H, 6.1; N, 5.5.

$[(L^{Me}H)V^{V}O]PF_6$ (3). A solution of vanadyl acetylacetonate, $VO(acac)_2$ (0.26 g; 1.0 mmol), and $L^{Me}H_3$ (0.54 g; 1.0 mmol) in acetone (30 mL) was heated to 40 °C with stirring for 30 min. Addition of solid $NaPF_6$ (0.7 g) to the solution initiated the precipitation of violet microcrystals. Yield: 0.24 g (32%). FAB MS (MNBA): *m*/*z* 596.7 {M^+}. Anal. Calcd for $C_{33}H_{43}N_3O_4PF_6V$: C, 53.4; H, 5.8; N, 5.7. Found: C, 53.2; H, 6.0; N, 5.7. $^{13}C\{^1H\}$ NMR (100 MHz, $CDCl_3$): δ 159.3, 151.2, 137.9, 133.5, 132.5, 132.1, 131.9, 130.3, 129.4, 128.3, 125.9, 124.9, 123.9, 123.6, 120.1, 118.6, 68.1, 64.8, 62.6, 62.0, 59.9, 57.0, 52.8, 50.5, 49.5, 21.4, 20.7, 20.6, 17.0, 16.8, 16.0 ppm.

$[L^{Bu}V^{IV}]PF_6$ (4). A deoxygenated solution of VCl_3 (0.16 g; 1.0 mmol) in CH_3CN (20 mL) was heated to reflux under an argon atmosphere until a clear green solution was obtained, to which $L^{Bu}H_3$ (0.78 g; 1.0 mmol) and a few drops of triethylamine were added. After addition of solid $NaPF_6$ (1.0 g) in the presence of air, black-violet microcrystals formed. Yield: 0.66 g (61%). μ_{eff}(293 K): 1.83 μ_B. FAB MS (MNBA): *m*/*z* 831.7 {$[M^+]$}. Anal. Calcd for $C_{51}H_{78}N_3O_3VPF_6$: C, 62.7; H, 8.0; N, 4.3. Found: C, 62.6; H, 8.3; N, 4.2.

$[L^{OCH_3}V^{IV}]PF_6$ (5). This complex was prepared as described above for **4** by using $L^{OCH_3}H_3$ (0.71 g; 1.0 mmol). The violet crude product was recrystallized from acetone. Yield: 0.32 (36%). Anal. Calcd for $C_{42}H_{60}F_6N_3O_6PV$: C, 56.1; H, 6.7; N, 4.7; V, 5.7. Found: C, 55.8; H, 6.8; N, 4.8; V, 5.5.

$[L^{Me}Co^{III}]$ (6). To a solution of $L^{Me}H_3$ (0.54 g; 1.0 mmol) in acetone (50 mL) were added $Co(CH_3CO_2)_2{\cdot}4H_2O$ (0.25 g; 1.0 mmol) and triethylamine (5 mL). The suspension was heated to reflux in the presence of air until a clear, deep green solution was obtained, from which, upon cooling, green microcrystals precipitated. Yield: 0.39 g (67%). FAB MS (MNBA): *m*/*z* 587.2 {$[M^+]$}. ^1H NMR (400 MHz, $CDCl_3$): δ 6.8 (s, 3H), 6.65 (s, 3H), 4.9 (d, 3H), 2.6−2.9 (m, 15H), 2.25 (s, 9H), 2.15 (s, 9H) ppm. Anal. Calcd for $C_{33}H_{42}N_3O_3Co$: C, 67.5; H, 7.2; N, 7.1. Found: C, 67.8; H, 7.4; N, 6.9.

$[L^{Bu}Co^{III}]$ (7). This complex was prepared as described above for **6** by using $L^{Bu}H_3$ (0.78 g; 1.0 mmol). Green microcrystals were obtained. Yield: 0.54 g (64%). FAB MS (MNBA): *m*/*z* 840.5 {$[M^+]$}. ^1H NMR (400 MHz, $CDCl_3$): δ 6.95 (d, 3H), 6.6 (d, 3H), 4.55 (d, 3H), 3.60 (m, 3H), 3.20 (m, 3H), 2.80 (d, 3H), 2.7 (m, 3H), 2.25 (m, 3H), 1.20 (s, 27H), 0.85 (s, 27H) ppm. Anal. Calcd for $C_{51}H_{78}N_3O_3Co$: C, 72.9; H, 9.4; N, 5.0. Found: C, 72.8; H, 10.0; N, 4.8.

$[L^{OCH_3}Co^{III}]$ (8). This complex was prepared as described above for **6** by using $L^{OCH_3}H_3$ (0.71 g; 1.0 mmol). Green-brown microcrystals were obtained. Yield: 0.56 g (66%). Electrospray ionization mass spectrum (positive ion): *m*/*z* 761 {$[M + H^+]$}. ^1H NMR (400 MHz, $CDCl_3$): δ 6.64 (d, J = 3.13 Hz, 3H), 6.23 (d, J = 3.13 Hz, 3H), 4.58 (d, J = 14.5 Hz, 3H), 3.68 (s, 9H), 3.51 (m, 3H), 3.21 (m, 3H), 2.76 (d, J = 14.5 Hz, 3H), 2.70 (m, 3H), 2.26 (m, 3H), 0.87 (s, 27H) ppm. $^{13}C\{^1H\}$ NMR (100 MHz, $CDCl_3$): δ 154.6, 148.1, 118.3, 113.9, 110.0, 62.8, 57.4, 56.5, 56.3, 34.8, 29.8, 14.5 ppm. Anal. Calcd for $C_{42}H_{60}N_3O_6Co$: C, 66.2; H, 7.9; N, 5.5; Co, 7.7. Found: C, 67.0; H, 8.0; N, 5.6; Co, 7.6.

(14) Halfen, J. A.; Young, V. G.; Tolman, W. B. *Angew. Chem., Int. Ed. Engl.* **1996**, *35*, 1687.

Table 1. Crystallographic Data for Complexes **9** and **10**

	9	**10**
formula	$C_{32}H_{55}ClCoN_3O_7$	$C_{35}H_{51}Cl_4CoN_4O_3$
fw	688.2	776.5
cryst syst	triclinic	monoclinic
space group	$P\bar{1}$	$P2_1/n$
a, Å	9.493(1)	10.184(2)
b, Å	9.760(1)	24.860(5)
c, Å	18.979(2)	14.872(3)
α, deg	88.57(1)	90
β, deg	78.60(1)	97.95(3)
γ, deg	79.24(1)	90
V, Å^3	1693.3(3)	3729.0(13)
Z	2	4
ρ_{calc}, g cm^{-3}	1.350	1.383
F(000)	736	1632
μ, mm^{-1}	0.635	0.79
cryst dimens, mm	0.73 × 0.42 × 0.14	0.28 × 0.46 × 0.70
λ, Å	0.710 73	0.710 73
T, K	100(2)	100(2)
no. of total data collected	14 832	14 718
no. of unique obsd data	6254 (R_{int} = 0.0639)	5354 (R_{int} = 0.0316)
no. of parameters refined	409	435
R^a	0.054	0.046
largest residual electron density, e Å^{-3}	0.86 (−0.60)	0.68 (−0.33)

^{a} $R = \sum(|F_o| - |F_c|)/\sum|F_o|$.

[L^{Pr}Co^{III}(acac)](ClO$_4$) (9). To a solution of the ligand L^{Pr}H (0.086 g; 0.2 mmol) in acetonitrile (10 mL) was added Co^{II}(acac)$_2$ (0.052 g; 0.2 mmol) in the presence of air. The solution was stirred at 20 °C for 1 h. Solid $NaClO_4$ (0.5 g) and H_2O (5 mL) were then added. The solution was allowed to stand at 0 °C for 12 h, during which red-brown microcrystals precipitated. Yield: 0.09 g (65%). ESI MS (positive ion; CH_3CN): *m*/*z* 588 {[L^{Pr}Co(acac)]$^+$}. ^{1}H NMR (400 MHz; $CDCl_3$): δ 7.02 (d, J = 2.4 Hz, 1H), 6.72 (d, J = 2.35 Hz, 1H), 5.56 (s, 1H), 4.48 (d, J = 14.2 Hz, 1H), 3.7−2.5 (m, 14H), 2.67 (d, J = 14.9 Hz, 1H), 2.23 (s, 3H), 1.73 (s, 3H), 1.60 (d, J = 6.4 Hz, 3H), 1.31 (s, 9H), 1.22 (s, 9H), 1.19 (d, J = 6.4 Hz, 3H), 1.14 (d, J = 6.4 Hz, 3H), 1.10 (d, J = 6.5 Hz, 3H) ppm. Anal. Calcd for $C_{32}H_{55}N_3O_7$-CoCl: C, 55.8; H, 8.1; N, 6.1. Found: C, 55.7; H, 7.9; N, 6.0.

[L^{Pr}Co^{III}(Cl$_4$cat)]·CH$_3$CN (10). To a solution of L^{Pr}H (0.043 g, 0.1 mmol) and N(Et)$_3$ (14 μL) in acetonitrile (5 mL) was added $CoCl_2$ (13 mg; 0.1 mmol). The solution was stirred at ambient temperature in the presence of air for 30 min. Tetrachlorocatechol (24 mg; 0.1 mmol) was added, and the solution was stirred for 1 h at 20 °C. Addition of water (5 mL) and cooling to 0 °C initiated the precipitation of aubergine microcrystals. Yield: 0.040 g (54%). FAB MS (dimethoxybenzyl alcohol matrix): *m*/*z* 734 {[L^{Pr}Co(Cl$_4$cat)]$^+$}. ^{1}H NMR (400 MHz; $CDCl_3$): δ 6.92 (d, J = 2.5 Hz, 1H), 6.67 (d, J = 2.4 Hz, 1H), 5.03 (d, J = 13.04 Hz, 1H), 3.85−2.2 (m, 14H), 2.93 (d, J = 13.18 Hz, 1H), 1.51 (s, 3H), 1.21 (s, 9H), 1.16 (d, J = 6.40 Hz, 3H), 1.10 (d, J = 6.38 Hz, 3H), 1.07 (s, 9H), 1.05 (d, J = 6.53 Hz, 3H) ppm. Anal. Calcd for $C_{33}H_{48}N_3O_3CoCl_4$·CH_3CN: C, 54.1; H, 6.6; N, 7.2. Found: C, 54.1; H, 6.4; N, 7.1.

X-ray Crystallography. Crystal data and data collection and refinement details are summarized in Table 1 (and corresponding tables in the Supporting Information). Graphite-monochromated Mo Kα X-radiation was used throughout. Intensities of a red-brown crystal of **9** and an aubergine crystal of **10** were collected at 100(2) K, respectively, by using the Siemens SMART system; they were corrected for Lorentz and polarization effects, but no corrections for absorption were carried out. The structures were solved by conventional Patterson and difference Fourier methods by using the Siemens SHELXTL-PLUS program package.[15] The function minimized during full-matrix least-squares refinement was $\sum w(|F_o| - |F_c|)^2$. All non-hydrogen atoms were refined anisotropically. The hydrogen atoms were placed at calculated positions and refined with isotropic thermal parameters.

Physical Measurements. Electronic spectra were recorded on a Perkin-Elmer Lambda 19 (range: 220−1400 nm) or on a Hewlett Packard HP 8452A diode array spectrophotometer (range: 220−820 nm). Cyclic voltammetry, square-wave voltammetry, and coulometric experiments were performed with EG&G equipment (Model 273A potentiostat/galvanostat). X-band EPR spectra of complexes in fluid solution at 298 K (10^{-3} M CH_3CN/CH_2Cl_2 solutions containing 0.10 M [TBA]PF_6 or [TBA]ClO_4) were measured on a Varian E-9 X-band spectrometer with 100 kHz modulation frequency at 298 K in a quartz cell (d = 0.3 mm). The data were digitized by means of a Stelar DS-EPR data station (Stelar snc, Mede, Italy). The spectra were simulated by iteration of the isotropic hyperfine coupling constants a and line widths $\Delta\nu_{1/2}$. We thank Dr. F. Neese (Abteilung Biologie der Universität Konstanz) for a copy of his EPR simulation program. Temperature-dependent measurements on frozen solutions of [**10**]$^{2\bullet 2+}$ in the range 3.5−150 K were carried out on a Bruker ESP 300E spectrometer equipped with an Oxford Instruments ESR 910 helium-flow cryostat with an ITC 503 temperature controller. Temperature stability was 0.2 K, and the temperature gradient across the sample was estimated to be less than 0.5 K. All NMR spectra were recorded on a 400 MHz Bruker AMX series spectrometer.

Resonance Raman spectra were recorded with a U1000 spectrograph (2400/mm holographic gratings) equipped with a liquid-nitrogen-cooled CCD detector (Instruments SA). The output of a dye laser (stilbene 3; Coherent 899-01) pumped by an argon ion laser (multiline UV; Coherent Innova 400) served as the excitation source. The laser power at the sample was about 50 mW. In order to avoid photoinduced degradation, the sample which exhibits an optical density of *ca*. 1.5 at the excitation wavelength was deposited in a rotating cell. The Raman scattered light was detected in 90° with a scrambler placed in front of the entrance slit of the spectrometer to account for the polarization sensitivity of the gratings. The spectral slit width was 2.8 cm^{-1}. The spectra, measured with an acquisition time of 15 s, were linearized in wavenumbers, yielding an increment of 0.24 cm^{-1} and a total spectral range of *ca*. 200 cm^{-1}. Thus, several spectra covering different but overlapping ranges are combined to give the overview spectra displayed in this work. In these spectra, the contributions of the solvent and the supporting electrolyte are subtracted.

Results

Synthesis of Complexes. Green microcrystals of [L^{Me}V^{III}] (**1**) precipitated slowly from an anaerobic reaction mixture of the ligand L^{Me}H$_3$ and VCl_3 in acetonitrile to which a few drops of triethylamine for deprotonation of the ligand had been added. Complex **1** was oxidized in methanol with $Na_2S_2O_8$. Upon addition of $NaPF_6$, violet crystals of [L^{Me}V^{IV}]PF_6 (**2**) were obtained. Both **1** and **2** are paramagnetic and display effective magnetic moments at 293 K of 2.89 μ_B (**1**) and 1.73 μ_B (**2**) indicative of octahedral vanadium(III) (d^2) and vanadium(IV) (d^1), respectively.

When V^{IV}O(acac)$_2$, where acac represents the monoanion pentane-2,4-dionate, was treated with 1 equiv of L^{Me}H$_3$ in acetone in the presence of air and $NaPF_6$ was added, violet microcrystals of [(L^{Me}H)V^{V}O]PF_6 (**3**) were obtained. Complex **3** is diamagnetic. In the IR spectrum, a sharp band at 947 cm^{-1} indicates the presence of a terminal oxo group (ν(V═O)). In the ^{1}H NMR spectrum, six well-resolved singlets in the range δ 2−2.5 are observed which are assigned to the protons of six chemically nonequivalent methyl groups. The ^{13}C NMR spectrum of **3** displays six methyl carbon signals at δ ∼20; in the range 50−70 ppm, nine resonances of the methylene carbon atom (ethyl and benzyl groups) are clearly detected, and of the expected 18 resonances of the aromatic carbon atoms, 16 are observed in the range 120−160 ppm. These data clearly indicate that all three pendent arms of the macrocyclic ligand [L^{Me}H]$^{2-}$ are different. We propose the structure for the monocation in **3**, shown in Chart 2, with two coordinated phenolates and one dangling phenol. In complexes **1** and **2**, the trianion [L^{Me}]$^{3-}$ is coordinated in an octahedral fashion to a V(III) and a V(IV) central ion, respectively. Here the three coordinated phenolate pendent arms are equivalent. We previ-

(15) Sheldrick, G. M. Full-matrix least-squares refinement package SHELX-TL-PLUS. Universität Göttingen, 1991.

Chart 2. Proposed Structures for **3** (left) and **4** (right)

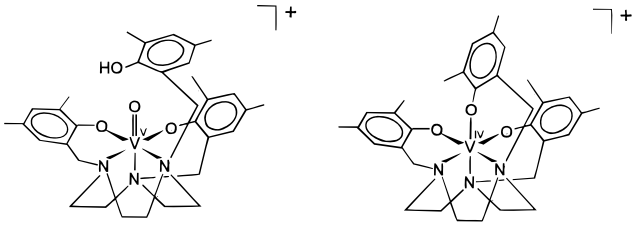

Table 2. Selected Bond Distances (Å) and Angles (deg) in **9** and **10**

	Complex **9**		
Co−O1	1.880(2)	Co−O2	1.887(2)
Co−O3	1.889(2)	Co−N1	1.948(2)
Co−N3	2.040(2)	Co−N2	2.040(3)
O3−C31	1.275(4)	O2−C29	1.281(4)
C30−C31	1.398(4)	O1−C9	1.345(3)
C29−C30	1.393(4)		
O1−Co−O2	92.83(9)	O1−Co−O3	89.93(8)
O2−Co−O3	92.07(9)	O1−Co−N1	88.96(9)
O2−Co−N1	87.94(9)	O3−Co−N1	178.89(9)
O1−Co−N3	176.40(9)	O2−Co−N3	89.85(9)
O3−Co−N3	92.37(9)	N1−Co−N3	88.73(10)
O1−Co−N2	89.59(9)	O2−Co−N2	174.68(9)
O3−Co−N2	92.67(9)	N1−Co−N2	87.36(10)
N3−Co−N2	87.54(9)		
	Complex **10**		
Co−O1	1.892(2)	Co−O2	1.897(2)
Co−O3	1.898(2)	Co−N1	1.949(2)
Co−N2	2.033(2)	Co−N3	2.059(2)
O2−C28	1.326(3)	O3−C29	1.316(3)
O1−C9	1.329(3)	C28−C29	1.422(4)
O1−Co−O2	88.61(8)	O1−Co−O3	85.79(8)
O2−Co−O3	86.67(8)	O1−Co−N1	95.67(8)
O2−Co−N1	89.89(9)	O3−Co−N1	176.23(9)
O1−Co−N2	89.24(8)	O2−Co−N2	176.96(8)
O3−Co−N2	95.32(9)	N1−Co−N2	88.18(9)
O1−Co−N3	175.54(8)	O2−Co−N3	95.33(8)
O3−Co−N3	92.34(8)	N1−Co−N3	86.44(9)
N2−Co−N3	86.90(9)		

ously reported[4] the crystal structure of an analogous complex $[LV^{IV}]BPh_4$, where L represents 1,4,7-tris(5-*tert*-butyl-2-hydroxybenzyl)-1,4,7-triazacyclononane.

By using the corresponding ligands $L^{Bu}H_3$ and $L^{OCH_3}H_3$ and similar reaction conditions as described above for the synthesis of **1**, we obtained, in the presence or absence of air, violet crystals of the vanadium(IV) complexes $[L^{Bu}V^{IV}]PF_6$ (**4**) and $[L^{OCH_3}V^{IV}]PF_6$ (**5**) as the only isolable products when $NaPF_6$ was added to the solution. Both compounds are paramagnetic with μ_{eff} at ∼1.7 μ_B. Figure S1 (Supporting Information) displays the X-band EPR spectrum of **5** in acetonitrile solution at 298 K. The observed ^{51}V hyperfine coupling constant of 1.07 mT ($g_{eff} = 1.99$) is very similar to those of other octahedral vanadium(IV) complexes[16] and proves that **5** is a genuine V(IV) species with a $3d^1$ electronic configuration. Note that **2**, **4**, and **5** do not exhibit a ν(V=O) stretching mode in the infrared in the range 900−1000 cm^{-1}.

Reaction of the pendent-arm macrocycles $L^{Me}H_3$, $L^{Bu}H_3$, and $L^{OCH_3}H_3$ with $Co^{II}(CH_3CO_2)_2 \cdot 4H_2O$ in acetone in the presence of air affords, upon addition of triethylamine, green microcrystals of the neutral complexes $[L^{Me}Co^{III}]$ (**6**), $[L^{Bu}Co^{III}]$ (**7**), and $[L^{OCH_3}Co^{III}]$ (**8**), respectively. The ^1H NMR spectra prove that the three pendent arms are equivalent in each of these

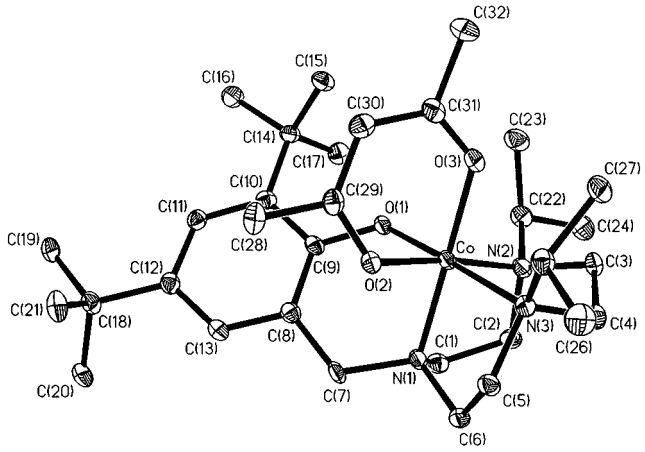

Figure 1. Perspective view of the monocation in crystals of **9**.

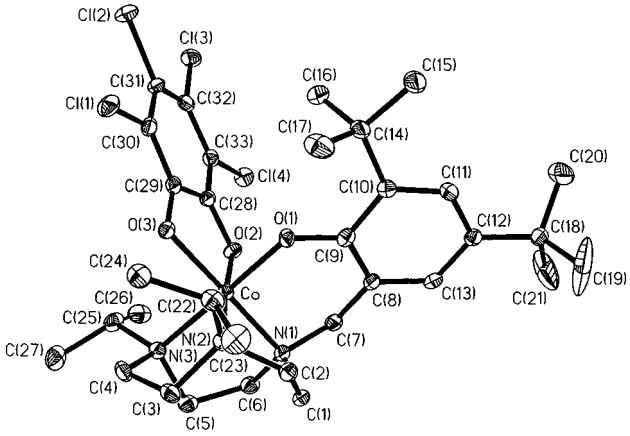

Figure 2. Perspective view of the neutral complex in crystals of **10**.

diamagnetic species. Therefore, we propose that the cobalt(III) (d^6 low spin) ions are in an octahedral environment comprising three facially bound amine nitrogen and three phenolate oxygen donors.

The ligand $L^{Pr}H$ is tetradentate and contains three tertiary amine nitrogen donors and one pendent phenol arm. Thus, the reaction of $L^{Pr}H$ with $Co^{II}(acac)_2$ in the presence of air in acetonitrile solution affords, upon addition of $NaClO_4$, red-brown microcrystals of $[L^{Pr}Co^{III}(acac)](ClO_4)$ (**9**). From a similar reaction of $CoCl_2$, $L^{Pr}H$, and tetrachlorocatechol (Cl_4-catH_2) in acetonitrile, aubergine microcrystals of the neutral diamagnetic complex $[L^{Pr}Co^{III}(Cl_4cat)]$ (**10**) were obtained.

Crystal Structures. The structures of **9** and **10** have been determined at 100(2) K by single-crystal X-ray crystallography. Figure 1 shows the structure of the monocation in crystals of **9**, and Figure 2, that of the neutral complex **10**. Selected bond distances and angles are summarized in Table 2.

In both mononuclear complexes, the cobalt ion is surrounded by a facial N_3O_3 donor set. The monoanionic ligand $[L^{Pr}]^-$ is tetradentate, and its pendent arm is coordinated as a phenolate. The average $Co-O_{phen}$ bond at 1.885 Å is very short in comparison with those of other known phenolate cobalt(III) species.[17] Two further coordination sites are occupied in **9** by a chelating pentane-2,4-dionate ligand and in **10** by a tetrachlorocatecholate. The average $C-O_{phenolate}$ bond at 1.337 Å in **9** and **10** and the average $C-O_{cat}$ bond at 1.321 Å in **10** indicate that the phenolate and tetrachlorocatecholate ligands prevail (and

(16) Mabbs, F. E.; Collison, D. *Studies in Inorganic Chemistry: Electron Paramagnetic Resonance of d Transition Metal Compounds*; Elsevier: Amsterdam, 1992; Vol. 16.

(17) Riley, P. E.; Pecoraro, V. L.; Carrano, C. J.; Raymond, K. N. *Inorg. Chem.* **1983**, *22*, 3096.

(18) Adams, D. M.; Dei, A.; Rheingold, A. L.; Hendrickson, D. N. *J. Am. Chem. Soc.* **1993**, *115*, 8221.

Table 3. Redox Potentials of the Complexes [a]

complex	solvent	$E^1_{1/2}$,V	$E^2_{1/2}$,V	$E^3_{1/2}$,V	$E^4_{1/2}$,V	$E^5_{1/2}$
1	CH_3CN			0.33	−0.55	
2	CH_3CN			0.33	−0.55	
3	CH_3CN		1.06 (irr)	−0.39		
4	CH_3CN			0.37	−0.49	
5	CH_3CN	1.38 (irr)	1.07 (irr)	0.13	−0.71	
$[L'V^{III}]$[b]				0.38	−0.50	−2.41
7	CH_2Cl_2	0.75	0.41	0.01		
8	CH_3CN	0.43	0.18	−0.10		
9	CH_3CN	0.46				
10	CH_3CN	0.62	0.16			

[a] Redox potentials, $E^x_{1/2} = (E_p^{ox} + E_p^{red})/2$, are referenced *vs* the ferrocenium/ferrocene (Fc^+/Fc) couple; for irreversible (irr) processes, peak potentials, E_p^{ox}, are given. Conditions: solvent containing 0.10 M [TBA]PF_6 or [TBA]ClO_4 supporting electrolyte; glassy carbon working electrode; Ag/AgCl (saturated $LiCl/C_2H_5OH$) reference electrode; scan rate 200 mV s^{-1}. [b] $L'H_3$ = 1,4,7-tris(5-*tert*-butyl-2-hydroxybenzyl)-1,4,7-triazacyclononane; ref 4.

not their phenoxyl or semiquinonate forms).[18] All Co−O distances in **9** and **10** are smaller than 1.90 Å. We take this as clear structural evidence that, at 100 K in the solid state, the cobalt ions are in the oxidation state +III and no valence isomers such as Co^{II}(semiquinonate) species are present.[19]

Electrochemistry. The electrochemistry of the complexes was investigated by cyclic and square-wave voltammetry and controlled-potential electrolysis (coulometry) of acetonitrile or dichloromethane solutions containing 0.10 M tetra-*n*-butylammonium hexafluorophosphate ([TBA]PF_6) as supporting electrolyte. All redox potentials are referenced to the ferrocenium/ferrocene couple (Fc^+/Fc); they are summarized in Table 3. Table 4 gives details of the electronic spectra of the complexes.

The cyclic voltammograms of the tris(phenolato)vanadium complexes **1**, **2**, **4**, and **5** are very similar; they display two reversible one-electron-transfer waves in the potential range −1.5 to +0.9 V *vs* Fc^+/Fc. The square-wave voltammogram of **5** shown in Figure S2 (Supporting Information) shows two additional, irreversible oxidation peaks at +1.07 and 1.38 V, which probably correspond to ligand-centered processes. The reversible electron transfer processes are assigned to metal-centered processes V^{III}/V^{IV} and V^{IV}/V^{V} as in eq 1. Stepwise

$$[LV^{V}]^{2+} \underset{-e}{\overset{+e}{\rightleftharpoons}} [LV^{IV}]^{+} \underset{-e}{\overset{+e}{\rightleftharpoons}} [LV^{III}] \qquad (1)$$

$$E^3_{1/2} \qquad E^4_{1/2}$$

$$L = [L^{Me}]^{3-}, [L^{Bu}]^{3-}, [L^{OCH_3}]^{3-}$$

controlled-potential electrolysis of **5** allows the spectroelectrochemical characterization of $[L^{OCH_3}V^{V}]^{2+}$, $[L^{OCH_3}V^{IV}]^{+}$, and $[L^{OCH_3}V^{III}]$. The UV−vis spectra of these species in CH_3CN solution are shown in Figure 3. In the visible region, the V^V and V^{IV} species exhibit intense phenolate-to-vanadium charge transfer bands which are shifted bathochromically with increasing oxidation state and increase in intensity at the same time. Note that the three spectra display an absorption *minimum* at 380−400 nm. Coordinated phenoxyl radical complexes display an intense maximum ($\epsilon > 4 \times 10^3$ L mol^{-1} cm^{-1}) in this region.[10,11,14] The absence of such maxima in the spectra of $[LV^{V}]^{2+}$ and $[LV^{IV}]^{+}$ supports therefore the assumption that the two successive one-electron oxidations of $[LV^{III}]$ are metal- rather than ligand-centered.

The CV (cyclic voltammogram) of the oxovanadium(V) species **3** shows one reversible one-electron-transfer wave at −0.39 V which is assigned to the V^V/V^{IV} couple. The enormous stabilization of the +V oxidation state by the presence of a terminal oxo group is well established in vanadyl coordination chemistry.[20]

The square-wave voltammogram of **7** and the CV of **8** both display *three* fully reversible one-electron-transfer waves. This is shown in Figure 4. Similar observations have been reported for the corresponding tris(phenolato) complexes of Ga^{III}, Sc^{III}, Cr^{III}, and Fe^{III}.[10] These oxidation processes are ligand-centered as in eq 2 and indicate that one, two, and three coordinated

$$[LCo^{III}]^{3+} \underset{-e}{\overset{+e}{\rightleftharpoons}} [LCo^{III}]^{2+} \underset{-e}{\overset{+e}{\rightleftharpoons}} [LCo^{III}]^{+} \underset{-e}{\overset{+e}{\rightleftharpoons}} [LCo^{III}] \qquad (2)$$

$$E^1_{1/2} \qquad E^2_{1/2} \qquad E^3_{1/2}$$

phenolates are successively oxidized to the corresponding phenoxyl radical. Thus, the trication $[LCo^{III}]^{3+}$ contains three coordinated phenoxyl ligands, whereas the dication has two phenoxyls and one phenolate and the monocation contains one phenoxyl and two phenolates. On the time scale of a coulometric experiment at −30 °C, only the monocations of **7** and **8** are stable enough to allow their spectroscopic characterization. In both cases, two new absorption maxima at ∼400 and >600 nm are observed for the monocations (Table 4 and Figure S3 (Supporting Information)). As we showed previously[10] for $[L^{OCH_3}Ga]^+$, $[L^{OCH_3}Sc]^+$ and $[L^{Bu}Ga]^+$, $[L^{Bu}Sc]^+$, as well as for the complexes $[L^{OCH_3}Fe]^+$ and $[L^{Bu}Fe]^+$, these bands are typical of coordinated phenoxyl radicals.

In a previous paper,[10] we reported a linear correlation between the redox potentials, $E^3_{1/2}$, of the $[L^{OCH_3}M^{III}]^+/[L^{OCH_3}M^{III}]$ couple (M = Sc, Fe, Cr) and the average O−M−O bond angle α. This angle is a measure for the extent of $M-O_{phenolate}$ *π-bonding* effects. A pronounced M═O double-bond character of the three phenolate-to-metal bonds (note: phenolates are good *π*-donors) induces an opening of this angle (α > 90°). Although we have not been able to determine α for **8**, it is reasonable to assume a value of 89−90°. This would be in line with the structure determinations of **9** and **10** and the fact that $Co-O_{phenolate}$ bonds are single bonds since the t_{2g} orbitals are filled and therefore they cannot accept oxygen-to-cobalt(III) *π bonding*. It is gratifying that the $E^3_{1/2}$ of **8** fits the above linear correlation at α ∼ 90° as is shown in Figure 5. Thus, the extent of M−O *π-bonding* tunes the redox potentials of the ligand-centered redox process. A potential range of ∼400 mV is observed for the $[L^{OCH_3}M^{III}]^+/[L^{OCH_3}M^{III}]$ couple on going from Co^{III} (no *π-bonding) to* Sc^{III} *(strong π-bonding)*.[10] We cannot offer a theoretical rationale for the observed linearity of this correlation at this point.

Complex **9** contains only one oxidizable coordinated phenolate group, and consequently, the CV of **9** (Figure S4 (Supporting Information)) displays only one reversible one-electron-transfer wave at 0.46 V in the potential range +0.9 to −0.20 V. At more negative potentials, an irreversible reduction at $E_{p,red}$ = −0.80 V is observed which we assign to a metal-centered reduction of the cobalt(III) to a labile cobalt(II) ion. Figure 6 (top) shows the spectral changes observed upon electrochemical one-electron oxidation of red-brown **9** yielding the paramagnetic violet dication $[L^{Pr}Co^{III}(acac)]^{\bullet 2+}$. The intense new absorption maxima at 405 and 545 nm indicate that a phenoxyl radical has been generated.

(19) (a) Buchanan, R. M.; Pierpont, C. G. *J. Am. Chem. Soc.* **1980**, *102*, 4951. (b) Adams, D. M.; Dei, A.; Rheingold, A. L.; Hendrickson, D. N. *Angew. Chem.* **1993**, *105*, 954; *Angew. Chem., Int. Ed. Engl.* **1993**, *32*, 880.

(20) Bonadies, J. A.; Carrano, C. J. *J. Am. Chem. Soc.* **1986**, *108*, 4088.

Table 4. Electronic Spectral Data for the Complexes

complex	solvent	λ_{max}, nm (ϵ, L mol^{-1} cm^{-1})
1	CH_3OH	576 (590), 380 sh, 271 (1.6×10^4), 216 (1.7×10^4)
2	CH_3OH	570 (1.4×10^4), 420 sh, 270 (1.9×10^4)
3	CH_3OH	575 (9.0×10^3), 420 (5.0×10^3), 274 (1.3×10^4), 217 (2.7×10^4)
4	CH_3OH	580 (7.5×10^3), 430 sh, 320 sh, 273 (1.5×10^4)
5	CH_3CN	634 (1.0×10^4), 459 (7.7×10^3), 324 sh, 282 (2.5×10^4), 252 (5.0×10^4)
6	CH_3OH	602 (1.0×10^3), 404 (1.4×10^3), 262 (2.9×10^4), 214 (2.9×10^4)
7	CH_2Cl_2	578 (480), 480 sh, 410 (3.1×10^3), 368 (2.9×10^3), 317 sh, 272 (2.7×10^4), 258 (2.6×10^4)
8	CH_3CN	592 (650), 450 sh, 380 (3.8×10^3), 330 sh, 320 sh, 278 (2.5×10^4), 254 sh
9	CH_3CN	699 (220), 490 (1.1×10^3), 289 (1.9×10^4), 241 (1.9×10^4)
10	CH_3CN	502 (800), 307 sh (1.7×10^4), 242 (3.9×10^4)
		Electrochemically Generated Complexes
$[L^{OCH_3}V^{III}]$	CH_3CN	609 (1.5×10^3), 392 sh, 287 (3.0×10^4), 252 (3.6×10^4)
$[L^{OCH_3}V^{V}]^{2+}$	CH_3CN	870 (3.2×10^4), 604 sh, 324 sh, 282 (2.6×10^4), 252 (5.2×10^4)
$[L^{Bu}Co^{III}]^{\bullet+}$ [b]	CH_2Cl_2	760 (1.4×10^3), 398 (4.8×10^3), 382 sh, 286 (2.4×10^4), 256 (2.1×10^4)
$[L^{OCH_3}Co^{III}]^{\bullet+}$ [a]	CH_3CN	678 (1.6×10^3), 418 sh, 402 (4.9×10^3), 288 (2.1×10^4), 246 (2.1×10^4)
$[\mathbf{9}]^{\bullet 2+}$	CH_3CN	545 (1.5×10^3), 405 (4.7×10^3), 304 (2.5×10^4), 270 sh (2.1×10^4), 240 sh (2.0×10^4)
$[\mathbf{10}]^{\bullet+}$	CH_3CN	641 (2.5×10^3), 426 (4.0×10^3), 406 (3.1×10^3), 327 (1.6×10^4), 244 (3.5×10^4)
$[\mathbf{10}]^{2\bullet 2+}$ [a]	CH_3CN	524 (4.3×10^3), 432 sh (4.5×10^3), 412 (7.2×10^3), 392 sh (5.2×10^3), 314 (2.8×10^4)

[a] Generated by controlled-potential electrolysis at −30 °C in CH_3CN (0.10 M $[TBA]PF_6$) solution or [b] in CH_2Cl_2.

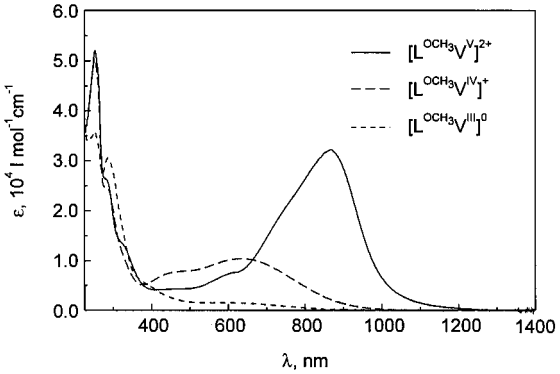

Figure 3. Electronic spectra of **5** and its electrochemically reduced $[L^{OCH_3}V^{III}]$ and oxidized $[L^{OCH_3}V^{V}]^{2+}$ forms in CH_3CN (0.10 M $[TBA]PF_6$).

Replacement of the redox-innocent acetylacetonate ligand in **9** by the dianionic tetrachlorocatecholate affording **10** has an interesting effect on the corresponding CV shown in Figure S4 (bottom). In the potential range +1.1 to −0.50 V, *two* reversible one-electron-transfer waves are observed, and at very negative potentials, an irreversible process is detected with $E_{p,red} = -1.3$ V and $E_{p,ox} = -0.70$ V, which is assigned to the Co^{III}/Co^{II} couple. Coulometric measurements established unambiguously that both reversible one-electron processes correspond to oxidations of **10**. Figure 6 (bottom) shows the electronic spectra of the parent complex **10**, as well as its one- and two-electron-oxidized forms, respectively. The two oxidized species were generated at controlled potentials of 0.35 and 0.8 V *vs* Fc^+/Fc, respectively, and their spectra were recorded in CH_3CN solution containing 0.10 M $[TBA]PF_6$. Oxidation of aubergine **10** to its monocation $[\mathbf{10}]^{\bullet+}$ is accompanied by a color change to blue-green. In the electrochemically generated paramagnetic monocation $[\mathbf{10}]^{\bullet+}$, either the catecholate is oxidized, to the corresponding semiquinonate *or* the phenolate is oxidized yielding a phenoxyl ligand. The electronic spectrum in conjunction with the EPR and resonance Raman spectra (see below) of $[\mathbf{10}]^{\bullet+}$ suggests that the catecholate ligand is oxidized to give the monocation $[L^{Pr}Co^{III}(Cl_4\text{-semiquinonate})]^{\bullet+}$. In the electronic spectrum of $[\mathbf{10}]^{\bullet+}$, three intense new absorption maxima at 406, 426, and 641 nm are observed which do not resemble the features in the spectrum of $[\mathbf{9}]^{\bullet 2+}$ containing a phenoxyl ligand. Further one-electron oxidation of $[\mathbf{10}]^{\bullet+}$ affording $[\mathbf{10}]^{2\bullet 2+}$ induces a dramatic change in the electronic spectrum, and a color change to violet is observed. A very intense absorption

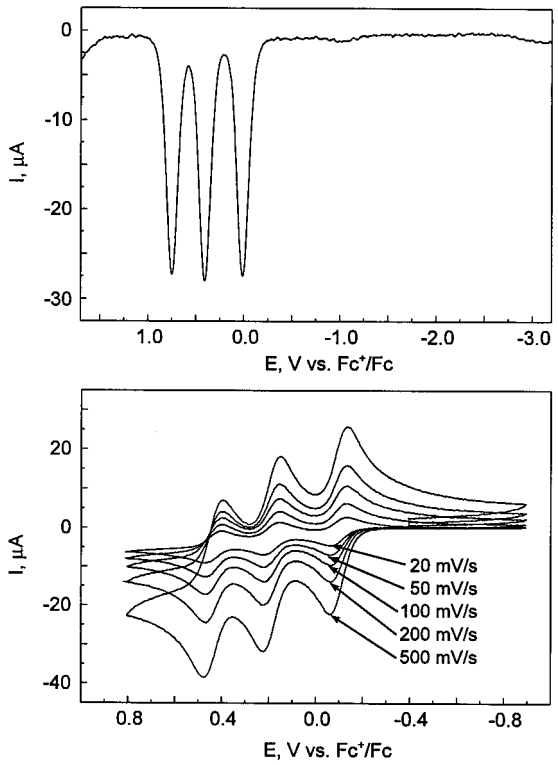

Figure 4. Square-wave voltammogram (top) in CH_2Cl_2 and cyclic voltammograms (bottom) in CH_3CN (0.10 M $[TBA]PF_6$) of **7** and **8**, respectively, at a glassy carbon working electrode.

maximum at 412 nm and one at ∼520 nm indicate that the phenolate has now been converted to a phenoxyl ligand. Thus, the dication $[\mathbf{10}]^{2\bullet 2+}$ contains a semiquinonate and a phenoxyl radical coordinated to a cobalt(III) ion.

EPR Spectroscopy. X-band EPR spectra of the electrochemically generated radical complexes $[\mathbf{9}]^{\bullet 2+}$, $[\mathbf{10}]^{\bullet+}$, and $[\mathbf{10}]^{2\bullet 2+}$ in CH_3CN solution containing 0.10 M $[TBA]PF_6$ or $[TBA]ClO_4$ supporting electrolyte are shown in Figure 7. Because of the short lifetime of electrochemically generated $[\mathbf{7}]^{\bullet+}$ and $[\mathbf{8}]^{\bullet+}$ at 20 °C, the EPR spectra were recorded at 77 K. Under these conditions, a broad unresolved signal at $g = 2.004$ (CH_3CN solution) indicative of the expected $S = {}^1/_2$ ground state was observed. These spectra are very similar to the spectrum reported for $[L^{OCH_3}Ga^{III}]^{\bullet+}$,[10] although the width of the signals is significantly broader than that of the latter. This is probably due to an unresolved ^{59}Co hyperfine splitting.

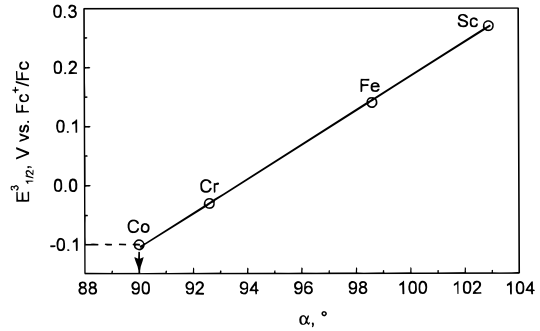

Figure 5. Correlation of the redox potentials, $E^3_{1/2}$, of the couples $[L^{OCH_3}M]^+/[L^{OCH_3}M]$ *versus* the $O_{phen}-M-O_{phen}$ bond angle α. This line is a linear regression.

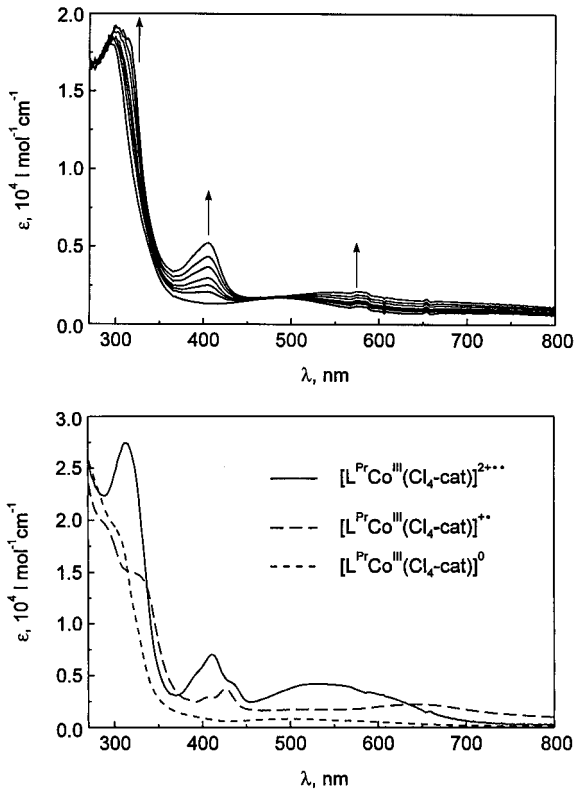

Figure 6. Top: Spectral changes observed during electrochemical one-electron oxidation of **9** in CH_3CN (0.10 M $[TBA]ClO_4$) at 20 °C. Bottom: Electronic spectra of **10** (20 °C) and electrochemically generated $[\mathbf{10}]^{+\bullet}$ (20 °C) and $[\mathbf{10}]^{2\bullet 2+}$ (−30 °C) in CH_3CN (0.10 M $[TBA]PF_6$).

The spectrum of $[\mathbf{9}]^{\bullet 2+}$ displays a signal at $g = 2.0047$. Hyperfine coupling to the ^{59}Co nucleus ($I = {}^7/_2$), $a_{Co} = 6.0$ G, and to one benzylic proton, $a_H = 6.55$ G, is detected. Using these parameters with a Gaussian line width of 2.27 G, the resulting simulation is shown in Figure 7a (dotted line). The spectrum clearly indicates the presence of a coordinated phenoxyl radical where the two benzylic protons are magnetically not equivalent (as in its reduced form **9**, for which the ^{1}H NMR spectrum shows two diastereotopic protons). The hyperfine splitting to the second benzylic proton and to the aromatic ring proton in a meta position is not resolved.

The spectrum of the corresponding radical $[\mathbf{10}]^{+\bullet}$ shown in Figure 7b shows a simple eight-line hyperfine pattern at $g = 2.0044$. The hyperfine splitting constant, a_{Co}, was determined to be 11.0 G. A simulation using this parameter and a Gaussian line width of 4.70 G is shown in Figure 7b (dotted line). Clearly, no hyperfine coupling to a benzylic proton is observed. We take this as good evidence that one-electron oxidation of

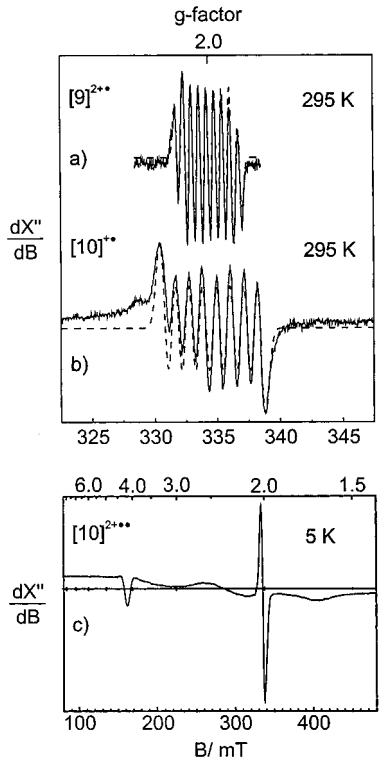

Figure 7. X-band EPR spectra of electrochemically generated (a) $[\mathbf{9}]^{\bullet 2+}$ at 295 K, (b) $[\mathbf{10}]^{+\bullet}$ at 295 K, and (c) $[\mathbf{10}]^{2\bullet 2+}$ at 5 K in CH_3CN solution. The dotted lines represent simulations with g values and hyperfine coupling constants given in the text. Microwave power: (a, b), 5 mW; (c) 1 mW. Modulation amplitude: (a, b), 0.3 mT; (c) 1.5 mT.

10 yields a (semiquinonato)cobalt(III) species. A number of such species have been characterized previously by EPR spectroscopy, and in all cases where the semiquinonate is coordinated to cobalt(III) as a didentate ligand, cobalt hyperfine coupling constants in the range 9−12 G have been reported.[19a,21−23]

X-band spectra of the diradical $[\mathbf{10}]^{2\bullet 2+}$, which was electrochemically prepared at −30 °C in acetonitrile solution (0.10 $[TBA]PF_6$), were measured in frozen solution only. The observed absorption derivative traces in the range 3−150 K are a superposition of two subspectra (Figure 7c): a very broad pattern in the field range 0−400 mT and a narrow isotropic resonance composed of eight weakly resolved hyperfine lines ($a = 20$ G) centered at $g = 2.0$. The prominent $g = 2$ line was the only detectable feature at room temperature, but its intensity was found to be sample-preparation dependent. Quantitation of this signal revealed in "bad" preparations 0.9 spin per molecule which decreased to 0.1 spin per molecule in the most elaborate, low-temperature preparations of $[\mathbf{10}]^{2\bullet 2+}$. Therefore, we discard this half-integer-spin signal and attribute it to $[\mathbf{10}]^{+\bullet}$ or to some other decomposition product.

The appearance of the broad subspectrum with two extremely broad lines at 270 and 400 mT in the vicinity of $g = 2$ and a narrow trough at $g = 4$ is typical of a spin-triplet spectrum with zero-field splitting on the order of the microwave quantum ($D \approx h\nu$; 0.3 cm^{-1} at X-band). The feature at $g = 4.12$ is then assigned to a $\Delta m = 2$ transition. The triplet character of the spectrum proves the presence of the diradical $[\mathbf{10}]^{2\bullet 2+}$, which

(21) Wicklund, P. A.; Beckmann, L. S.; Brown, D. G. *Inorg. Chem.* **1976**, *15*, 1996.
(22) Kessel, S. L.; Emberson, R. M.; Debrunner, P.; Hendrickson, D. N. *Inorg. Chem.* **1980**, *19*, 1170.
(23) Lange, C. W.; Conklin, B. J.; Pierpont, C. G. *Inorg. Chem.* **1994**, *33*, 1276.

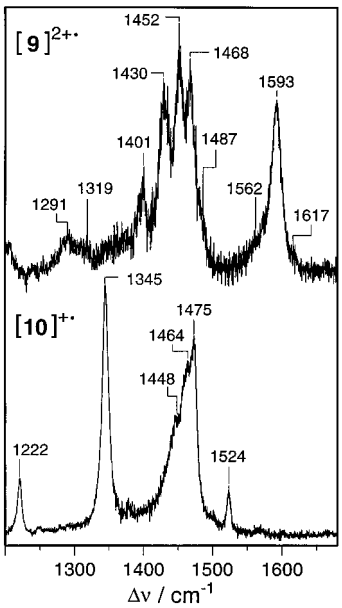

Figure 8. Resonance Raman spectra of electrochemically generated $[\mathbf{9}]^{\bullet 2+}$ (top) and $[\mathbf{10}]^{\bullet +}$ (bottom) in CH_3CN (0.10 M $[TBA]ClO_4$ and $[TBA]PF_6$, respectively) at 298 K (λ_{exc} = 427 nm).

exhibits intramolecular spin coupling. This broad spectrum was observed from 2.8 to 150 K without significant changes in line shape. From the variation of the intensity as a function of the temperature, as was determined from single integrations of the trough signal at $g = 4.12$ in the range 6−120 K with 50 μW power, the singlet−triplet splitting of the diradical was estimated to be +24 (±10) cm^{-1}. This energy value indicates an intramolecular ferromagnetic coupling of the semiquinonate and the phenoxyl radical with a coupling constant $J = +12$ (±5) cm^{-1} using the spin-Hamiltonian $H = -2JS_{semiquin}\cdot S_{phenoxyl}$ ($S_{semiquin} = S_{phenoxyl} = {}^1/_2$). It is interesting to note that in tris(semiquinonato)cobalt(III) complexes the semiquinonate−semiquinonate coupling has been found to be antiferromagnetic.[23] An $S = {}^1/_2$ ground state has been observed.

Resonance Raman (RR) Spectra. Figure 8 displays the RR spectra of electrochemically generated species $[\mathbf{9}]^{\bullet 2+}$ and of $[\mathbf{10}]^{\bullet +}$ in acetonitrile solution (0.10 M $[TBA]PF_6$ or $[TBA]ClO_4$) recorded with excitation at 427 nm in resonance with the corresponding absorption maxima of both species shown in Figure 6.

The spectrum of $[\mathbf{9}]^{\bullet 2+}$ exhibits features at 1593, 1468, 1452, 1430, and 1401 cm^{-1}. The band at 1593 cm^{-1} is readily assigned to the C=C stretching mode (ν_{8a}), which in uncoordinated phenoxyl radicals is found at 1585 cm^{-1} (2,4-dimethylphenoxyl)[24] but in phenoxyl−metal complexes is found at higher frequencies.[11,25] Hence, the 7 cm^{-1} upshift in the spectrum of $[\mathbf{9}]^{\bullet 2+}$ points to a coordinated phenoxyl radical. Further support of this notion comes from the behavior of the C−O stretching mode ν_{7a} and its RR intensity relative to that of the ν_{8a} mode. For free phenoxyl radicals the ν(C−O) vibration is found above ~1510 cm^{-1},[26] with an approximately 10-fold intensity compared to that of the ν_{8a} mode. Upon coordination to a metal ion, this mode shifts to lower frequencies and the ν_{7a}/ν_{8a} intensity ratio is nearly reversed.[11,25] The RR spectrum of $[\mathbf{9}]^{\bullet 2+}$ reveals no intense band at ~1510 cm^{-1}, but a weak shoulder of the 1468 cm^{-1} peak at 1487 cm^{-1} is attributable to the ν_{7a} mode. Its low intensity as well as its frequency separation relative to the ν_{8a} mode of 125 cm^{-1} is consistent with previous findings on coordinated phenoxyl radicals.[11,25] In this respect, the spectrum of $[\mathbf{9}]^{\bullet 2+}$ resembles those of related phenoxyl−metal complexes, but the relative RR intensities of the bands at 1468, 1452, 1430, and 1401 cm^{-1} are significantly stronger than those observed previously. This effect may be due to the differing resonance conditions. In the present case, the RR spectra were excited at the low-energy side of the phenoxyl $\pi \rightarrow \pi^*$ transition whereas the other spectra were recorded with excitation at the high-energy side.[27]

It is important that the RR spectrum of $[\mathbf{10}]^{\bullet +}$ does not resemble that of $[\mathbf{9}]^{\bullet 2+}$. The observed features at 1524, 1475, 1464 (sh), 1345, and 1222 cm^{-1} do not correspond to vibrations of a coordinated phenoxyl radical. We assign these frequencies to modes of a coordinated tetrachlorosemiquinonate, where the band at 1524 cm^{-1} is due to a C−O stretching frequency, in agreement with previous IR spectroscopic measurements on *p*-semiquinonates.[22,28] Tripathi et al. have also shown that this mode dominates the RR spectrum of a *m*-semiquinonate radical.[29] Presumably, this intensity distribution is similar for *o*-semiquinonates. Regardless of a detailed assignment of all observed bands, it can be safely concluded that the monocation $[\mathbf{10}]^{\bullet +}$ does not contain a phenoxyl ligand.

Discussion

Octahedral tris(phenolato)metal complexes containing the pendent-arm macrocyclic ligands $[L^{Me}]^{3-}$, $[L^{Bu}]^{3-}$, and $[L^{OCH_3}]^{3-}$ display a rich and diverse redox chemistry even when the central metal ion itself is redox inactive, *e.g.* Sc^{III}, Ga^{III}, or Zn^{II}.[10,11,25] It has been shown that in the latter instances the coordinated phenolates undergo reversible one-electron oxidations yielding coordinated phenoxyl species provided that the ortho and para positions of the aromatic rings are protected by sterically demanding groups such as a *tert*-butyl or methoxy group. Note that two methyl groups in these positions on each ring as in $[L^{Me}]^{3-}$ are not sufficient to stabilize the phenoxyl radicals.[30] For instance, the CV of $[L^{Me}Sc^{III}]$ in CH_3CN displays two *irreversible* oxidation waves at quite anodic potentials, whereas for the corresponding complexes $[L^{Bu}Sc^{III}]$ and $[L^{OCH_3}Sc^{III}]$ three *reversible* one-electron-transfer waves in the same potential range have been reported, respectively.[10]

The situation in the above cases is quite clear and unequivocal; *i.e.*, the UV−vis, EPR, and RR spectra of the corresponding monocations $[LM]^{\bullet +}$ with an $S = {}^1/_2$ ground state clearly demonstrate the presence of one coordinated phenoxyl radical.[10,11,25] If the central metal ion is a transition metal with a d^n (n is >1 but <10) electron configuration, it is not *a priori* possible to discern one-, two-, and three one-electron oxidations between ligand- and metal-centered processes and each case has to be carefully assessed by spectroscopy (or, if possible, by crystallography).

An interesting example in this respect is the complex $[L^{OCH_3}Cr^{III}]$, which undergoes three reversible, successive one-electron-

(24) (a) McGlashen, M. L.; Eads, D. D.; Spiro, T. G.; Whittaker, J. W. *J. Phys. Chem.* **1995**, *99*, 4918. (b) Mukherjee, A.; McGlashen, M. L.; Spiro, T. G. *J. Phys. Chem.* **1995**, *99*, 4912.
(25) Sokolowski, A.; Leutbecher, H.; Weyhermüller, T.; Schnepf, R.; Bothe, E.; Bill, E.; Hildebrandt, P.; Wieghardt, K. *J. Biol. Inorg. Chem.*, in press.
(26) (a) Chipman, D. M.; Liu, R.; Zhou, R.; Pulay, P. *J. Chem. Phys.* **1994**, *7*, 5023. (b) Johnson, C. R.; Ludwig, M.; Asher, S. A. *J. Am. Chem. Soc.* **1986**, *108*, 905. (c) Tripathi, G. N. R.; Schuler, R. H. *J. Phys. Chem.* **1988**, *92*, 5129.
(27) Tripathi, G. N. R.; Schuler, R. H. *J. Chem. Phys.* **1984**, *81*, 113.
(28) Matsunaga, Y. *J. Chem. Phys.* **1964**, *41*, 1609.
(29) (a) Tripathi, G. N. R.; Chipman, D. M.; Miderski, C. H.; Davis, H. F.; Fessenden, R. W.; Schuler, R. H. *J. Phys. Chem.* **1986**, *90*, 3968. (b) Tripathi, G. N. R. In *Time Resolved Spectroscopy*; Clark, R. J. H., Hester, R. E., Eds.; John Wiley and Sons: New York, 1989; p 184.
(30) Altwicker, E. R. *Chem. Rev.* **1967**, *67*, 475.
(31) Sokolowski, A.; Bothe, E.; Bill, E.; Weyhermüller, T.; Wieghardt, K. *J. Chem. Soc., Chem. Commun.* **1996**, 1671.

transfer oxidations yielding a mono-, di-, and tricationic species. $[L^{OCH_3}Cr](ClO_4)$ has been characterized by X-ray crystallography.[31] It was established that it contains two coordinated phenolates, one coordinated phenoxyl radical, and a chromium(III) ion. The metrical details of the phenolate and phenoxyl ligands differ significantly, and gratifyingly, the experimentally observed C−C and C−O distances of the phenoxyl radical in $[L^{OCH_3}Cr^{III}]^{\bullet+}$ agree nicely with those reported for phenoxyl and tyrosyl from density functional calculations.[32]

In contrast, one-electron oxidation of $[L'V^{III}]$, where L′ represents 1,4,7-tris(5-*tert*-butyl-2-hydroxybenzyl)-1,4,7-triazacyclononane, also yields a monocation but the crystal structure of $[L'V]BPh_4$ shows unambiguously that the monocation contains three equivalent coordinated phenolates and a central V^{IV}. In this case, clearly, a metal-centered oxidation prevails.[4] The present study on the analogous complexes **1**, **2**, **4**, and **5** underlines this point. The UV−vis spectral changes observed on going from V^{III} to V^{IV} to V^{V} cannot be accounted for by involving ligand-centered phenoxyl formation. All the data available point to metal-centered redox processes.

The cobalt(III) complexes **7** and **8**, on the other hand, display three reversible one-electron-transfer steps yielding mono-, di-, and trications, respectively. The monocations $[\mathbf{7}]^{\bullet+}$ and $[\mathbf{8}]^{\bullet+}$ are stable enough in solution at −30 °C to allow their spectroscopic characterization. Both possess an $S = {}^1/_2$ ground state, as was established by their EPR spectra. The UV−vis spectra of these species demonstrate that a coordinated phenoxyl ligand is present. Thus, the oxidation state +IV for the central cobalt ion is not accessible in the potential range investigated.

Complexes **9** and **10** represent interesting cases because the latter contains two different oxidizable ligands, namely a coordinated phenolate and a catecholate ligand. Species $[\mathbf{9}]^{\bullet+}$ shows the spectroscopic features of a coordinated phenoxyl radical whereas the monooxidized form of **10**, namely $[\mathbf{10}]^{\bullet+}$, shows features in the EPR and RR spectrum typical of a coordinated semiquinonate ligand. These spectral characteristics of a bound phenoxyl and a semiquinonate differ significantly and allow their unequivocal identification. It is also of significance that the two ligand radicals in $[\mathbf{10}]^{2\bullet2+}$ (each with $S = {}^1/_2$) are intramolecularly ferromagnetically coupled, yielding an $S = 1$ ground state. This type of coupling is most probably due to the fact that the two magnetic orbitals are orthogonal in the dication diradical.

Acknowledgment. We thank the Fonds der Chemischen Industrie for financial support Professor Y. Sasaki for granting a leave of absence to A.K. P.H. is grateful to the Deutsche Forschungsgemeinschaft for a Heisenberg stipend.

Supporting Information Available: Figure S1, showing the EPR spectrum of **5**, Figure S2, displaying the square-wave voltammogram of **5**, Figure S3, exhibiting the spectral changes observed upon one-electron oxidation of **7** and **8**, respectively, Figure S4, showing the cyclic voltammograms of **9** and **10**, and tables of crystallographic and structure refinement data, atom coordinates and U_{eq} values, bond lengths and angles, anisotropic thermal parameters, and calculated positional parameters of hydrogen atoms for complexes **9** and **10** (17 pages). Ordering information is given on any current masthead page.

IC970256E

(32) Qin, Y.; Wheeler, R. A. *J. Am. Chem. Soc.* **1995**, *117*, 6083.